

Cylindrical piezoelectric mobile actuator based on travelling wave

R. Bansevicius*, G. Kulvietis**, D. Mazeika**, A. Drukteinienė**, A. Grigoravicius**

*Kaunas University of Technology, Kęstučio 27, 44312 Kaunas, Lithuania, E-mail: bansevicius@cr.ktu.lt

**Vilnius Gediminas Technical University, Sauletekio 11, 10223 Vilnius, Lithuania,

E-mail: Genadijus_Kulvietis@gama.vtu.lt, Dalius.Mazeika@sc.vgtu.lt, astad@it.su.lt, arturas.grigoravicius@gmail.com

crossref <http://dx.doi.org/10.5755/j01.mech.18.5.2698>

1. Introduction

Piezoelectric actuators are widely used for high precision mechanical systems such as positioning devices, manipulating systems, control equipment and etc [1, 2]. Piezoelectric actuators have advanced features such as high resolution, short response time, compact size, and good controllability [1, 2]. Many design principles of piezoelectric actuators are proposed and used [3].

The piezoelectricity in such a material may be due to several effects, thus research into the mechanism of piezoelectricity and the enhancement of activity by new forming and poling processes and synthetic methods is still required [4].

Summarizing its all the following types of piezoelectric actuators can be specified: traveling wave, standing wave, hybrid transducer, and multimode vibrations actuators [2, 5].

Piezoelectric actuators have advanced features compare to others and are widely used for different commercial applications [1, 5]. A lot of design and operating principles are investigated to transform mechanical vibrations of piezoceramic elements into elliptical movement of the contact zone of actuator [2, 3, 6, 7]. Traveling wave piezoelectric actuators fall under two types – rotary and linear. Rotary type actuators are one of the most popular because of high torque density at low speed, high holding torque, quick response and simple construction. Linear type traveling wave actuators feature these advantages as well but development of these actuators is complex problem [8].

In general many design principles of piezoelectric actuators are proposed. Summarizing the following types of piezoelectric actuators can be specified: traveling wave, standing wave, hybrid transducer, and multimode vibrations actuators.

Piezoelectric actuator of upper traveling wave type is presented and analyzed in this paper.

2. Design and operating principle of piezoelectric actuator

The model of a piezoelectric actuator is composed of cylinder made of PZT-8 piezoceramic material (Fig. 1). The polarization vector is directed along the width of the cylinder. The detailed properties of this material are provided in Table 1.

Sinusoidal voltage with the different phase shifted by $2\pi/3$ is applied on each piezoceramic element.

Travelling wave is generated in the upside of the cylinder when axial type oscillations are applied. In general case several waves can be generated, but we narrow

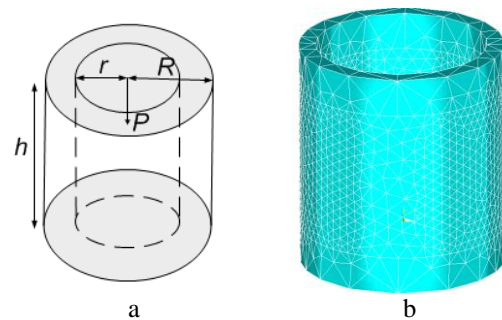


Fig. 1 Piezoelectric cylinder: a – principle scheme of a piezoelectric actuator, where P – the vector of polarization, R – outer radius, r – inner radius, h – height; b – finite element model of the cylindrical actuator and vibration mode of the actuator at 62 kHz

Table 1

The properties of the material used for modeling

Material property	Piezoceramics PZT-8
Jung modulus N/m^2	8.2764×10^{10}
Puason coefficient	0.33
Density kg/m^3	7600
Dielectric permittivity $\times 10^3 \text{F/m}$	$\epsilon_{11} = 1.2; \epsilon_{22} = 1.2; \epsilon_{33} = 1.1$
Piezoelectric matrix $\times 10^{-3} \text{C/m}^2$	$e_{13} = -13.6; e_{23} = -13.6;$
	$e_{33} = 27.1; e_{42} = 37.0;$
	$e_{51} = 37.0$

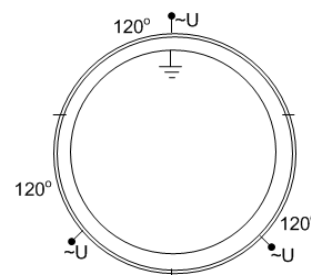


Fig. 2 The scheme of electrode placement

down to one wave.

In the electrode configuration diagram (Fig. 2) electrode plates are attached to the outer cylinder planes every other 120° degrees. Altogether three electrode plates are attached. Grounded is the inner cylinder plate.

Connecting the electrodes to the electrical current and grounding according to above-described electrode configuration a travelling wave at the top of the cylinder is created.

3. The influence of geometric parameters on domination coefficients

During numerical analysis as only geometric parameters of actuators change, the problem of the change in the sequence of eigenforms arises, and that means that an unsuitable eigenvalue can be chosen on the level of the scheme for determining rational geometric parameters Fig. 2. Since vibration equipment usually functions in one of its eigenfrequencies, as the sequence of eigenforms changes the solution usually does not converge, and numerical analysis becomes meaningless.

Usually, for numerical analysis of piezoactuators the software such as ANSYS is used. By the algorithm of eigenvalue problem eigenfrequencies for the systems are sorted in the ascending order; thereby the sequences of eigenforms change. This rule for sorting frequencies is disadvantageous when numerical analysis of multidimensional piezoactuators needs to be automated. This problem is also important for optimization, since calculations are tied both to eigenfrequencies and eigenforms. If the eigenfrequency is chosen incorrectly, the piezoactuator will not function, so it is very important to numerically determine eigenforms and place them inside the eigenform matrix of the construction model [9].

The authors propose for a given construction to calculate eigenfrequencies and forms of the construction. Then for the n th eigenfrequency the following sum can be formed

$$S_k^n = \sum_{i=1}^r (A_{ik}^n)^2, \quad r = \frac{l}{k} \quad (1)$$

where k is the number of degrees of freedom in a node, l is the number of nodes (degrees of freedom) in the model, r is the size of the form vector for the k th coordinate, A_{ik}^n is the value of the eigenform vector for the i th element. Then the ratio is formed

$$m_{jk}^n = \frac{S_j^n}{S_k^n}, \quad j \neq k \quad (2)$$

where m_{jk}^n is the oscillation domination coefficient. The sum S_k^n corresponds to the oscillation energy of the n th eigenfrequency in the k th direction, and the ratio m_{jk}^n is the ratio of oscillation energies of the n th eigenfrequency in the coordinate directions of j and k .

These coefficients have to be called partial domination coefficients since they estimate energy only in two coordinate directions. The domination coefficients discussed above have the following shortcomings.

Not normalized. Because of this the range of the domination coefficients calculated vary from 0 to infinity.

In the case of three dimensions, six domination coefficients result. Such a number of coefficients aggravate analysis.

To solve this problem the following algorithm is proposed: find the sum of the amplitude squares of piezoactuator oscillations in all directions of the degrees of freedom for a point, i.e., the full system energy in all directions [10, 11]

$$S_k^n = \sum_{i=1}^r (A_{ik}^n)^2 \quad (3)$$

where n is the eigen frequency for the system, k is the number of degrees of freedom in a node, A_{ik}^n is the value of the eigenform vector for the i th element.

Then the ratio is calculated [11]

$$m_j^n = \frac{S_j^n}{\sum_{i=1}^k S_i^n} \quad (4)$$

where m_j^n is the oscillation domination coefficient corresponds to the n th eigenform. The index j of domination coefficients indicates, in which direction the energy under investigation is the largest. j can assume such values: 1 corresponds to the x coordinate, 2 – y , and 3 – z , etc. Having calculated domination coefficients in all directions of degrees of freedom and having compared them to each other, we can determine the dominant oscillation type. The domination coefficients calculated according to formula (4) are normalized, so their limits vary from 0 to 1. It is very convenient for analyzing the influence of various parameters on domination coefficients.

To clearly determine the eigenform and its place in the eigenform matrix of the construction model, it is not enough to calculate only the oscillation domination coefficients. Domination coefficients only help to differentiate eigenforms by dominating oscillations, for example, radial, tangential, axial, etc.

Because of this an additional criterion is introduced into the process of determining eigenform, individual for each eigenform, i.e., the number of nodal points or nodal lines for the form. That depends on the dimensionality of the eigenform. During calculations the number of nodal points of beam-like and two-dimensional piezoactuators is determined by the number of sign changes in oscillation amplitude for the full length of the piezoactuator in the directions of coordinate axes.

Summarizing the algorithm for determining eigenforms of piezoactuator oscillations, we can note that it is composed of two integral stages: calculating domination coefficients and determining the number of nodal points or lines of the eigenform. This algorithm is not tightly bound to multidimensional piezoactuators, so it can be successfully applied in analysing oscillations of any constructions. When solving dynamics problems of piezoactuators for high precision microrobots where repeated calculations with higher eigenfrequencies are involved, it is proposed to modify the general algorithm introducing the stage of determining eigenforms with the help of domination coefficients [10].

4. Results of numerical modeling

Numerical modeling of piezoelectric actuator was performed to validate actuator design and operating principle through the modal and harmonic response analysis.

Recent applications of the piezoelectric finite elements were directed towards techniques of post processing. Precisely by recommended simplifications, they consist on using standard finite elements to calculate me-

chanical displacements, then to deduce the electric entities (potential, load) by post processing [12].

FEM software ANSYS 11.0 was employed for the simulation and FEM model was built (Fig. 1). PZT-8 piezoceramic was used for the cylinder. Dimensions of piezoelectric cylinder were set to $(D \times d \times h)$: $50 \times 35 \times 20$ mm.

Modal analysis of piezoelectric actuator was performed to find proper resonance frequency. Material damping was assumed in the finite element model. No structural boundary conditions were applied.

During analysis the dimensions of cylinders height have been changed. Geometric parameters proportions used in the finite element modal analysis are $R/h = 0.5$; $R/h = 1$; $R/h = 1.5$; $R/h = 2$ (Fig. 3). For each case considered an eigenvalue problem has been solved and harmonic analysis performed; the amplitudes for the contact point, and the system eigenfrequencies have been calculated for each construction considered.

The detailed measurements of geometric parameters are provided in Table 2.

Domination coefficients (Fig. 4) and eigenfrequencies (Fig. 5) have been also calculated. A more detailed analysis is provided below.

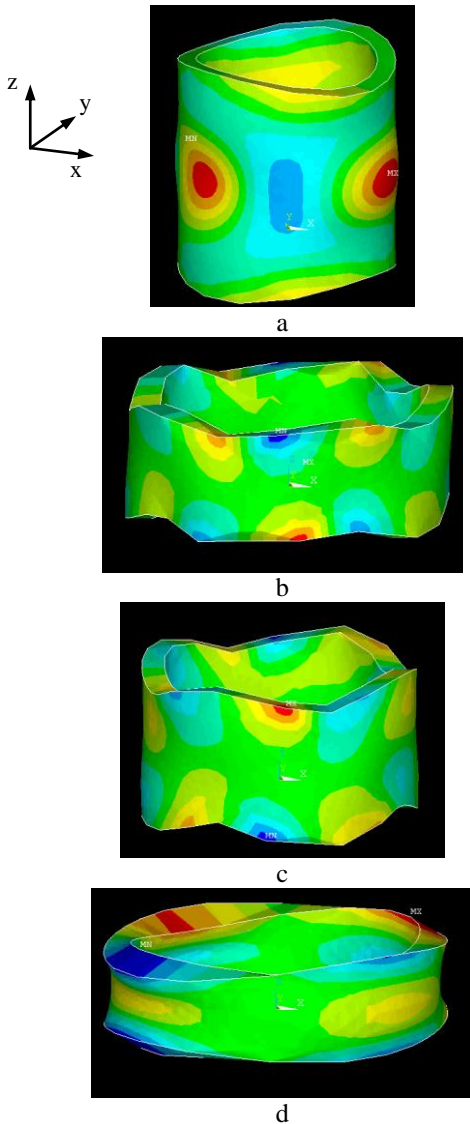


Fig. 3 Finite element models of the cylindrical actuators: a) $R/h = 0.5$; b) $R/h = 1$; c) $R/h = 1.5$; d) $R/h = 2$

Table 2

The detailed measurement of geometric parameters

	Measurement of cylindrical actuator			
	$R/h = 0.5$	$R/h = 1$	$R/h = 1.5$	$R/h = 2$
Outer radius R , m	0.015	0.015	0.015	0.015
Inner radius r , m	0.0125	0.0125	0.0125	0.0125
Height h , m	0.03	0.015	0.01	0.0075

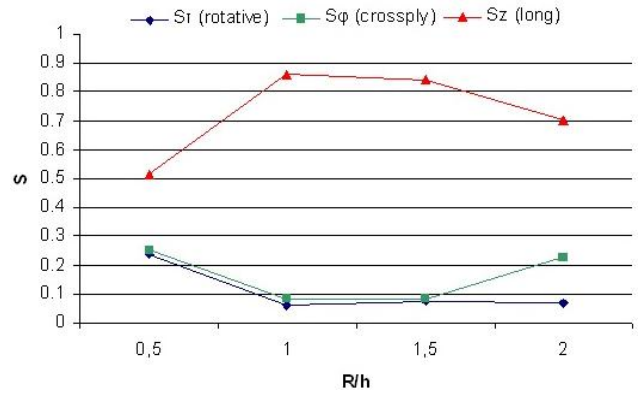


Fig. 4 The influence of geometric parameters on domination coefficients when geometric parameters proportions

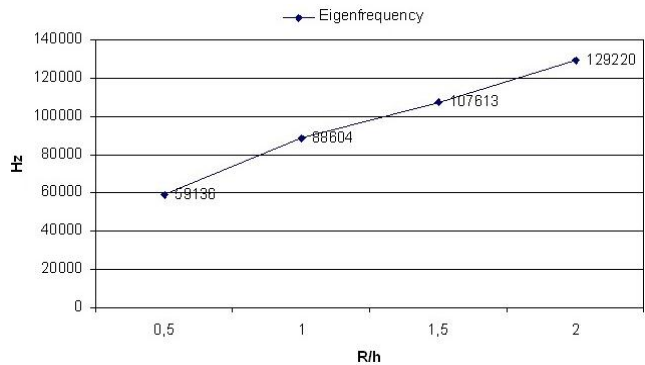


Fig. 5 The influence of geometric parameters on eigenfrequencies when geometric parameters proportions

The largest domination coefficients (Fig. 4) are in the y, z directions, and that means that flexional oscillations dominate.

Having compared the influence of geometric parameters on domination coefficients (Fig. 4) and eigenfrequencies (Fig. 5), we can claim that with the help of domination coefficients we can partially determine the eigenform of traveling wave.

Harmonic response analysis was performed with the aims to find out the actuator's response to sinusoidal voltage applied on electrodes of the piezoceramic elements, to verify operating principle. Analyzing oscillation characteristics travelling wave vibrations on the upside cylinder of the actuator will be manifested.

Compound parameters of the ellipses, i. e. dependencies of the ratio of major and minor axis and rotation of major axis are given in Table 3, Table 4.

Calculations in Table 3, Table 4 can be used to define operating frequency of actuator based on parameters of the ellipses.

Table 3
Trajectories dependencies of rotation of major axis are given when used schemes Fig. 2 to generate traveling wave

kHz	Angle (deg) by x axis			
	1	2	3	4
23.4	22.43	84.4	22.3	64.14
35.4	78.81	84.47	81.48	81.29
48.8	70.44	85.06	75.71	68.28
	Angle (deg) by y axis			
	1	2	3	4
23.4	79.7	23.54	81.06	22.7
35.4	70.37	61.14	70.82	62.76
48.8	80.86	79.33	87.14	71.49

Table 4
Trajectories dependencies of the ratio of major and minor axis are given when the schemes in Fig. 2 are used to generate traveling wave

kHz	Ratio by x axis			
	1	2	3	4
23.4	5.82	2.22	5.18	1.82
35.4	5.73	2.68	4.39	2.07
48.8	5.27	2.06	3.92	1.69
	Ratio by y axis			
	1	2	3	4
23.4	1.55	2.46	1.52	2.23
35.4	1.83	2.33	1.82	2.37
48.8	1.55	2.29	1.44	2.43

By observing elliptical trajectories of the contact point motion and their parameters it can be concluded that the trajectories has opposite directions at different frequencies. It means that slider will have direct and reverse motion at these frequencies.

Analyzing ellipsis parameters at axis x, bigger ratios are at 1st and 3rd points, while at axis y bigger ratios are at 2nd and 4th points.

Ellipsis at 35.4 kHz has larger major semiaxis and bigger area then at 23.4 kHz and 48.8 kHz (Fig. 6).

5. Geometric path-planning algorithm for cylindrical piezoelectric mobile actuator

This cylindrical piezoelectric actuator construction can be used not only for vibromotors, but also as a moving in two-dimensional space piezorobot (Fig. 7).

Two electrodes exciting schemes are used for the excitation of piezoelectric actuator.

1. One electrode sector is excited at a time, which generates rectilinear motion in XY plane.

2. All three electrode sectors are excited at a time with a phase difference 120° . In this case piezorobot will rotate around its central axis. Rotation can be clockwise and counterclockwise.

Using these two excitation schemes the path-planning algorithm was developed. Problem is analyzed

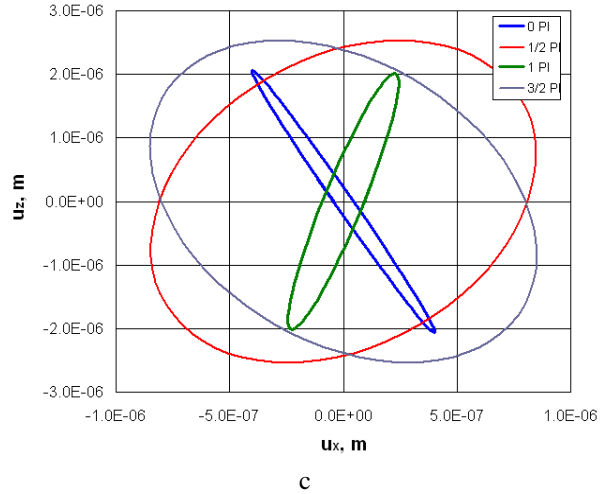
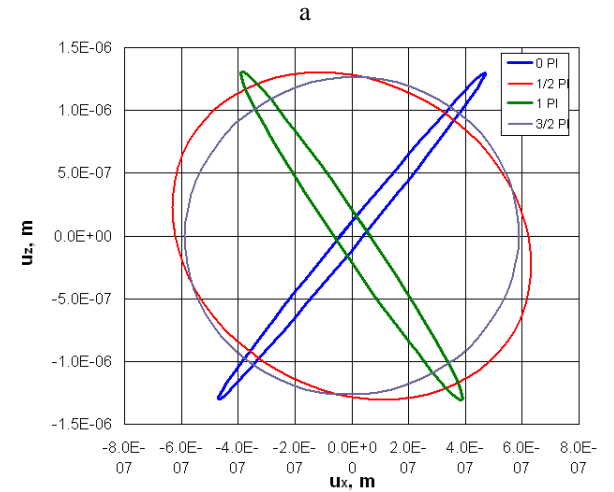
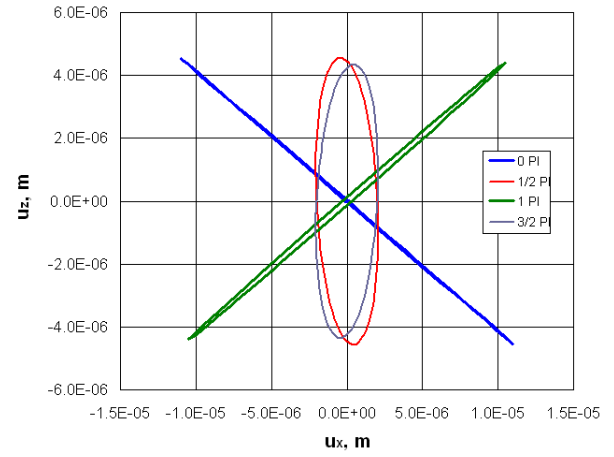


Fig. 6 Trajectories of the contact point motion by: U_x , U_z and U_y , U_z axis direction, the schemes in Fig. 2 are used to generate traveling wave, when resonant oscillations: a) 23.4 kHz; b) 35.4 kHz; c) 48.8 kHz

when original trajectory is curve, which is formatted between given points $(x_0; y_0)$, $(x_1; y_1)$, $(x_i; y_i)$, $(x_{i+1}; y_{i+1})$..., $(x_N; y_N)$, where $N \geq 2$. Curve functions are cubic splines in parametric form

$$S_i(S_{x_i}, S_{y_i}) = \begin{cases} S_{x_i} = \phi(x_i, x_{i+1}, t) \\ S_{y_i} = \psi(y_i, y_{i+1}, t) \end{cases} \quad (5)$$

where t is parameter of parametric function.

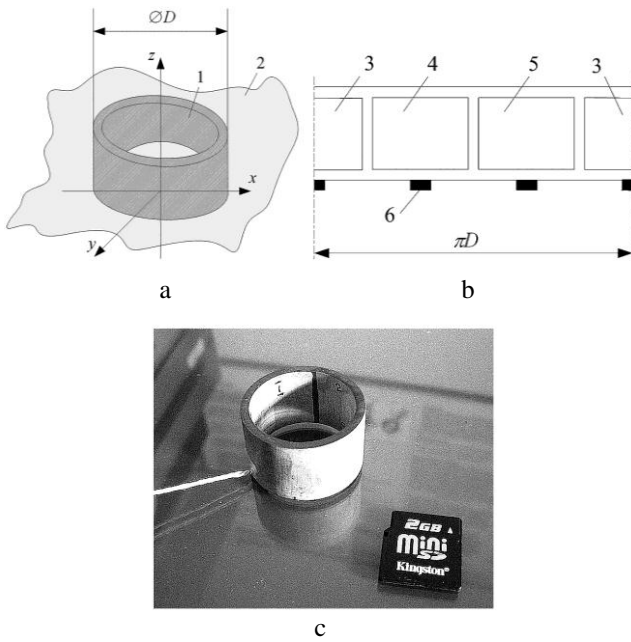


Fig. 7 Piezoelectric cylinder: (a) general scheme; (b) cylinder's outer surface of the involutes; (c) made from CTS-23 ceramic; 1 - cylinder piezoelectric and the radial polarization of the electrodes formed on the outer and inner surfaces of the cylinder, 2 - passive plane, 3-5 - electrode configuration, 6 - actuator's contact

Table 5

Piezorobot control data

j	c	$\theta, ^\circ$	D^*	x_r	y_r
1	1, 2, 3	39.7354	2	0	1
2	3	0	0	0.5723	0.78869
3	1, 2, 3	34.0234	1	0.5723	0.78869
4	3	0	0	0.96018	0.2491
5	1, 2, 3	26.6327	1	0.96018	0.2491
6	3	0	0	1	0
7	1, 2, 3	30.6562	2	1	0
8	1	0	0	0.78869	-0.5723
9	1, 2, 3	34.0234	1	0.78869	-0.5723
10	1	0	0	0.2491	-0.96018
11	1, 2, 3	26.6327	1	0.2491	-0.96018
12	1	0	0	0	-1
13	1, 2, 3	29.3437	1	0	-1
14	1	0	0	-0.57231	-0.78869
15	1, 2, 3	34.0234	1	-0.57231	-0.78869
16	1	0	0	-0.96018	-0.24915
17	1, 2, 3	26.6327	1	-0.96018	-0.24915
18	1	0	0	-1	0
19	1, 2, 3	30.6562	2	-1	0
20	2	0	0	-0.78869	0.5723
21	1, 2, 3	34.0234	1	-0.78869	0.5723
22	2	0	0	-0.24915	0.96018
23	1, 2, 3	26.6327	1	-0.24915	0.96018
24	2	0	0	0	1

1 - clockwise, 2 - counterclockwise

The main requirement for motion path is that the center of piezorobot would be at minimum distance from the original trajectory S_i . Thus, accuracy would be the maximum deviation from this trajectory.

Geometric path-planning algorithm:

Initial data: ε - maximum deviation from the

function, α_0 - angle between the first electrode segment and x axis.

1. First, determine whether the piezorobot can move from itself point $(x_{rj}; y_{rj})$ to a given point $(x_{i+1}; y_{i+1})$, i. e. it must be determined, whether a straight line $L(t)$ between these points does not cross the threshold of coordinates $g(\varepsilon, S)$ [13]. Solving the system of equations were calculating the intersection points $(x_g; y_g)$:

$$\begin{cases} x_g = g_{xi}(\varepsilon, S_{xi}(t_g)); \\ y_g = g_{yi}(\varepsilon, S_{yi}(t_g)); \\ x_g = L_{xj}(t_L); \\ y_g = L_{yj}(t_L). \end{cases} \quad (6)$$

where, t_g, t_L are parameters of parametric functions.

2. Calculating intersection points quantity Q .
3. Checked whether the condition $Q \leq 1$ is satisfied:
 - a. If it is true, then $x_{rj+1} = x_{i+1}, y_{rj+1} = y_{i+1}$.
 - b. Else:
 - b.1. Calculating tangent point $(x_T; y_T)$ at marginal coordinates [14]

$$\begin{cases} x_T = g_{xi}(\varepsilon, S_{xi}(t_g)); \\ y_T = g_{yi}(\varepsilon, S_{yi}(t_g)) \\ T(x_T, y_T, S_i(t_T)) = 0. \end{cases} \quad (7)$$

where T is equation of the tangent.

- b.2. Calculating piezorobot movement coordinates between three points

$$\frac{x_{rj+1} - x_{rj}}{x_{Ti} - x_{rj}} = \frac{y_{rj+1} - y_{rj}}{y_{Ti} - y_{rj}} \quad (8)$$

4. Go to the next original trajectory function $i = i + 1$.
5. Steps 1-4 are repeating until the final goal will be reached.
6. Then straight line orientation angle of the x-axis against can be calculate [14]

$$A_{Lj} = \arctg \frac{y_{rj+1} - y_{rj}}{x_{j+1} - x_{rj}} \quad (9)$$

7. Calculate piezorobot rotation angle for each power actuator, when the piezorobot is rotating clockwise [15]

$$360^\circ + \gamma_c(\alpha_j) - A_{Lj} \equiv \theta_{c1} \pmod{360} \quad (10)$$

and counter clockwise

$$360^\circ - \gamma_c(\alpha_j) + A_{Lj} \equiv \theta_{c2} \pmod{360} \quad (11)$$

where γ_c are angles between each piezoelectric actuator and x axis, c is piezoelectric actuators number.

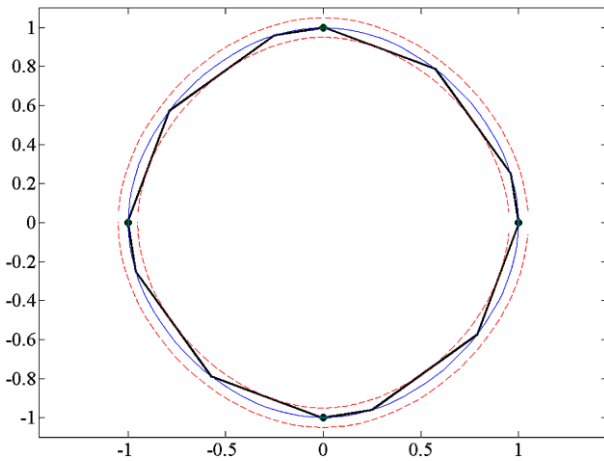


Fig. 8 Geometric path-planning with tangents method, when $\varepsilon = 0.05$ and $\alpha = 60^\circ$

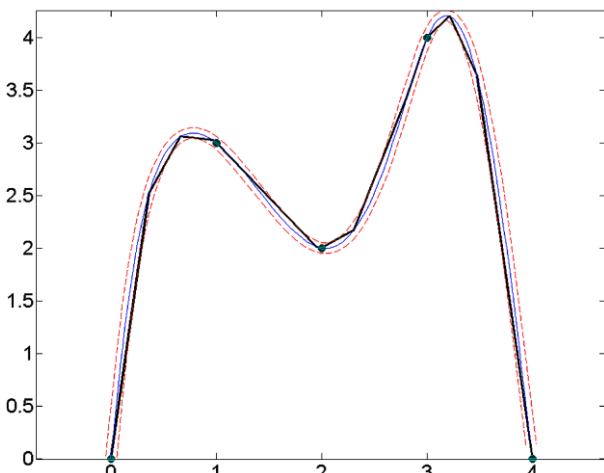


Fig. 9 Example of open trajectory path-planning

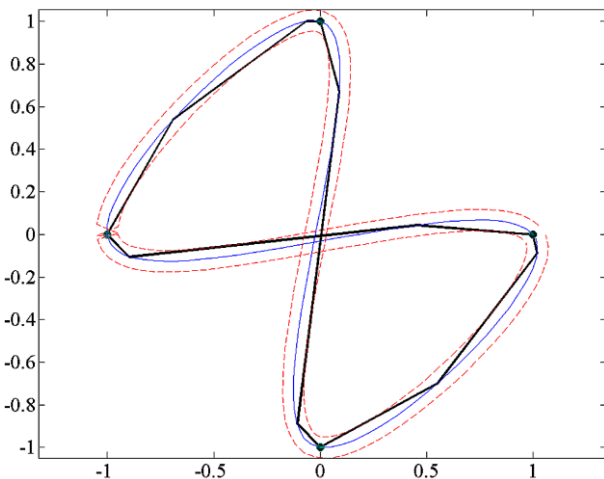


Fig. 10 Example of loop trajectory path-planning

8. Piezorobot turning angle will be $\theta_{min} = \min(\theta)$.
9. By this value place in the matrix θ can be determined turn direction (by column number) and which power actuator must be active to move on (by row number).
10. Go to the next straight line coordinates $j = j + 1$.
11. Recalculating $\alpha_j(\theta_{min})$.
12. Steps 7-11 are repeated until all piezorobot rotating angles are found.

After the completion of the tangents algorithm is

available the following data: coordinates of the motion ($x_r; y_r$), activated contact numbers (c), size of the rotation angle (θ), rotation direction (D). These data can be used in piezorobot control development.

Numerical experiment results are shown in Fig. 8 and in Table 5. Other numerical experiment results with different trajectories are shown in Figs. 9 and 10.

6. Conclusions

Results of numerical modeling and simulation of piezoelectric actuator of upper traveling wave type is presented and analyzed in this paper.

In numerical modeling part modal and harmonic analyses were performed, domination coefficients, eigenfrequencies calculated, elliptical trajectories of the contact point motion presented.

Elliptic trajectories of the four arbitrary points of the top surface of the actuators were calculated and travelling wave oscillations were shown.

Experimental studies confirmed that travelling wave oscillations were obtained on the top surface of the actuator.

Acknowledgement

This work has been supported by Research Council of Lithuania, Project No. MIP-122/2010.

References

1. Uchino, K.; Giniewicz, J. 2003. Micromechatronics, Marcel Dekker Inc, New York.
2. Bansevičius, R.; Barauskas, R.; Kulvietis, G.; Ragulskis, K. 1988. Vibromotors for Precision Micro-robots. Hemisphere Publishing Corp., USA.
3. Uchino, K. 1998. Piezoelectric ultrasonic motors: overview, Journal of Smart Materials and Structures 7: 273-285.
<http://dx.doi.org/10.1088/0964-1726/7/3/002>.
4. Ostaševičius, V.; Milašauskaitė, I.; Daukševičius, R.; Baltrušaitis, V.; Grigaliūnas, V.; Prosyčevas, I. 2010. Experimental characterization of material structure of piezoelectric PVDF polymer, Mechanika 6(86): 78-82.
5. Sashida, T.; Kenjo, T. 1994. An Introduction to Ultrasonic Motors, Oxford Press.
6. Bansevičius, R.; Kulvietis, G.; Mazeika, D. 2008. Piezoelectric wide range laser deflecting/scanning devices with one and two degrees-of-freedom: state of the art and latest developments, Proceedings of 11th Int. Conference "Actuator 08": 117-120.
7. Hemsel, T.; Wallaschek, J. 2000. Survey of the present state of the art of piezoelectric linear motors, Ultrasonics 38: 37-40.
[http://dx.doi.org/10.1016/S0041-624X\(99\)00143-2](http://dx.doi.org/10.1016/S0041-624X(99)00143-2).
8. Friend, J.; Nakamura, K.; Ueha, S. 2005. A travelling-wave linear piezoelectric actuator with enclosed piezoelectric elements – the "Scream" actuator, Proceedings of the 2005 IEEE/ASME International Conference on Advanced Intelligent Mechatronics Monterey: 183-188.
9. Allik, H.; Hugdes, T. 1970. Finite element method for piezoelectric vibrations, International Journal for Nu-

- meric Methods in Engineering 2: 151-157.
<http://dx.doi.org/10.1002/nme.1620020202>.
10. **Tumasonienė I.** 2009. Determining eigenforms of piezo actuators used in high-precision microrobots: summary of doctoral dissertation, Vilnius Gediminas Technical University, Vilnius: Technika, 24 p.
 11. **Tumasonienė, I.; Kulvietis, G.; Mažeika, D.; Bansevičius, R.** 2007. The eigenvalue problem and its relevance to the optimal configuration of electrodes for ultrasound actuators, *Journal of Sound and Vibration* 308: 683-691.
<http://dx.doi.org/10.1016/j.jsv.2007.04.036>.
 12. **Rahmoune, M.; Osmon, D.** 2010. Classic finite elements for simulation of piezoelectric smart structures, *Mechanika* 6(86): 50-57.
 13. **Bansevicius, R.; Drukteinienė, A.; Kulvietis, G.; Mažeika, D.** 2010. Switching leg method for trajectory planning of mobile piezobot, *J. of Vibroengineering* 12(1): 26-33.
 14. **Bansevicius, R.; Drukteinienė, A.; Kulvietis, G.** 2009. Trajectory planning method of rotating mobile piezobot, *J. of Vibroengineering* 11(4): 690-696.
 15. **Bansevicius, R.; Drukteinienė, A.; Kulvietis, G.** 2010. Adaptive moving algorithm of mobile piezobot. *Proceedings of the 16th International Conference on Information and Software Technologies*, ISSN 2029-0063.

R. Bansevicius, G. Kulvietis, D. Mažeika, A. Drukteinienė, A. Grigoravičius

CILINDRINIS PJEZOELEKTRINIS JUDESIO KEITIKLIS, VEIKIANTIS BĖGANČIOSIOS BANGOS PRINCIPU

R e z i u m ė

Straipsnyje pateikiama cilindrinio pjezoelektrinio judesio keitiklio konstrukcija, analizuojami jo veikimo principai. Keitiklio paviršiuje žadinant harmoninius skirtingų fazių svyravimus generuojama bėgančioji banga. Judesio keitiklio elektrodai žadinami harmonine įtampa, kurios fazių skirtumas $2\pi/3$. Baigtinių elementų metodu atliktas skaitinis eksperimentas, siekiant nustatyti rezonansinius dažnius, keitiklio savąsias formas bei apskaičiuoti viršutinių kontaktų taškų judesio trajektorijas. Pristatytas cilindrinio pjezoelektrinio keitiklio judesio trajektorijos formavimo algoritmas.

R. Bansevicius, G. Kulvietis, D. Mažeika, A. Drukteinienė, A. Grigoravičius

CYLINDRICAL PIEZOELECTRIC MOBILE ACTUATOR BASED ON TRAVELLING WAVE

S u m m a r y

A design of cylindrical type piezoelectric mobile actuator is proposed and analyzed in the paper. Traveling wave is generated on the top area of the actuator applying harmonic oscillations with different phases. Electrodes of piezoceramic elements are excited by harmonic voltage with phase difference of $2\pi/3$. Numerical modeling based on finite element method was performed to find resonant frequencies and modal shapes of the actuator and to calculate the trajectories of the upper points movements under excitation scheme. Path-Planning algorithm presented for cylindrical piezoelectric mobile actuator.

Keywords: piezoelectric cylinder, traveling wave, finite element modeling, path-planning algorithm.

Received April 12, 2011

Accepted October 12, 2012